small
NANO MICRO

Fabrication of Nanofluidic Biochips with Nanochannels for Applications in DNA Analysis

Deying Xia, Juchao Yan, and Shifeng Hou*

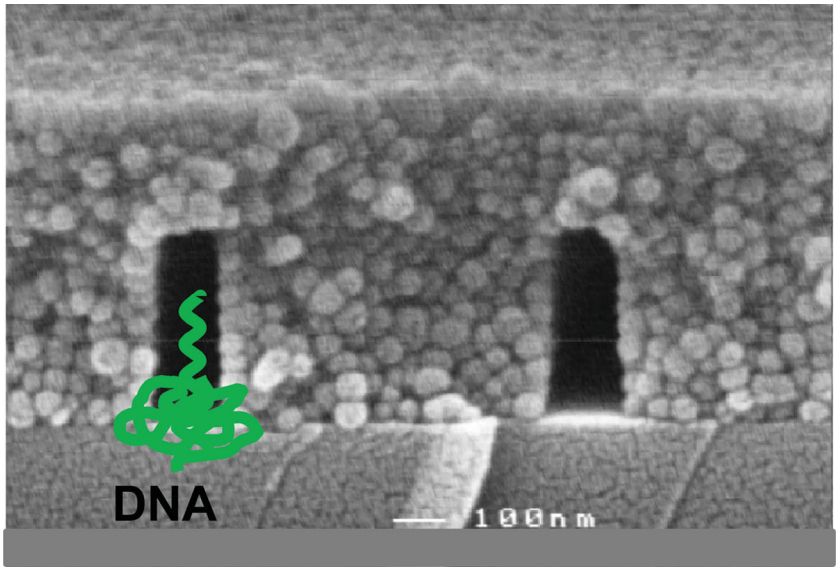

From the Contents

With the development of nanotechnology, great progress has been made in the fabrication of nanochannels. Nanofluidic biochips based on nanochannel structures allow biomolecule transport, bioseparation, and biodetection. The domain applications of nanofluidic biochips with nanochannels are DNA stretching and separation. In this Review, the general fabrication methods for nanochannel structures and their applications in DNA analysis are discussed. These representative fabrication approaches include conventional photolithography, interference lithography, electron-beam lithography, nanoimprint lithography and polymer nanochannels. Other nanofabrication methods used to fabricate unique nanochannels, including sub-10-nm nanochannels, single nanochannels, and vertical nanochannels, are also mentioned. These nanofabrication methods provide an effective way to form nanoscale channel structures for nanofluidics and biosensor devices for DNA separation, detection, and sensing. The broad applications of nanochannels and future perspectives are also discussed.

DOI: 10.1002/smll.201200240

1. Introduction

With the advancement of nanotechnology in recent years, many types of nanostructures have been successfully fabricated and demonstrated for use in a wide range of applications.[1] Important applications for these nanostructures are in chemical sensors and biosensors. Nanostructures can increase device specificity with surface functionalization methods to improve detection sensitivity with high surface areas and to speed up sample delivery with nanofluidic techniques.[2,3] Over the past decade, 1D nanostructures have been intensively studied for the detection of various biological molecules.[4–6] Nanochannels provide promising frameworks for optical detection in applications such as DNA separation, preconcentration and mapping. Nanochannels can be fabricated on site of the substrates and are easy to integrate the final detection devices with other components, thus having fewer processing procedures, lower cost and higher sensitivity. Though there has been much progress in fabricating nanochannels for biosensors, we are still facing various challenges, such as sensitivity, selectivity, stability and integration issues for the routine fabrication of cost-effective and scalable biosensors.[7] In this review article, we focus on nanochannel-based nanofluidic biosensors, especially for their use in DNA analysis.

In general, nanochannels are defined as channels that have at least one dimension in the range of 1 to 100 nm. Some researchers also use the term nanochannels to describe channels in the range of 100 nm to 1 μm. Three types of nanochannels are illustrated in **Figure 1**.[8] The first type is the low aspect ratio (AR) or planar nanochannel (also referred to as a nanoslit). The aspect ratio for a given channel is the ratio of the height to the width. Planar nanochannels can be fabricated using a combination of standard photolithography on the micro-scale in width and well-defined thin film deposition and etching in the vertical direction on the nano-scale. Numerous nanofluidic devices with planar nanochannels (nanoslits) have been fabricated due to the ease of fabrication and testing. The large width dimension of planar nanochannels is advantageous because it can yield a high flow rate, which results in ease of operation and detection. Currently, planar nanochannels still play an important role in the research of nanofluidics and in biosensing applications. The second type of nanochannel is the square nanochannel, which as an AR that is close to 1. This type of nanochannel represents the majority of nanochannels that have been fabricated in recent years. Various types of square nanochannels have been developed because of the rapid development in nanofabrication technologies. The third type of nanochannel is the deep nanochannel, which has a large AR. Deep nanochannels typically require more advanced and complicated nanofabrication techniques. There are relatively few reported nanofluidic biosensors based on deep nanochannels. Deep nanochannels are advantageous because they allow a higher level of integration and a higher throughput than low AR nanochannels. In addition, it should be noted that it is difficult to maintain an ideal rectangular or square shape in a cross sectional view of real fabricated nanochannels. Most nanochannels have an irregular, non-ideal shape; sometimes this shape is circular, triangular or trapezoidal.

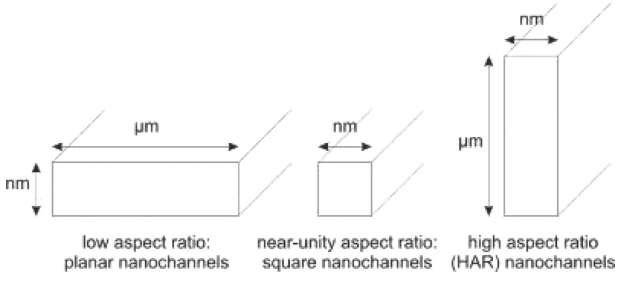

Figure 1. Planar (nanoslit), square, and deep nanochannels.[8] Copyright 2008, American Chemical Society.

Briefly, nanochannels could also be classified as a single nanochannel or an array of nanochannels in devices. An array of nanochannels can be easily fabricated and is always arranged into parallel lines. Cross-linked parallel nanochannels that are in the same level comprise the two-dimensional (2D) post matrix, which is used for the separation and detection of biomolecules. Most nanochannel devices are sealed on the top surface using different binding or fabrication techniques; however, it is possible to have open, deep nanochannel devices for easy access and operation.

Nanochannel devices have been rapidly developed because they can provide an ideal platform for investigating new fundamental phenomena as well as physics and chemistry principles in the nanoscale (e.g., new fundamental flow physics,[9] the concentration polarization behavior in nanochannels, and new theories and principles that govern transport in nanochannel devices[10]). Additionally, chemical reactions, synthetic chemistry and protein dynamics in nanochannels are different in nanochannels from their large channel analogues.[11] Different electrochemical phenomena emerge in nanochannels, which are used for the further development of smart electrochemical nanofluidic devices.[12]

Because the dimension of nanochannels is on the size order of biomolecules, these unique features provide the excellent control of transport, separation and detection of biomolecules. In contrast, gel electrophoresis, which was traditionally used for DNA detection, use porous media that is less well defined with limited pore sizes and poor mechanical properties. The applied electrical field direction and the dimension of nanochannels give precise control over the separation of certain sizes of DNA.[13] Nanofluidic

Dr. D. Xia
Department of Materials Science and Engineering
Massachusetts Institute of Technology
77 Massachusetts Avenue, Cambridge, MA 02139, USA
E-mail: dyxia@mit.edu
Prof. J. Yan
Department of Physical Sciences
Eastern New Mexico University
1500 S Avenue K, Portales, NM 88130, USA
Prof. S. Hou
Department of Chemistry & Biochemistry
Montclair State University
1 Normal Avenue, Montclair, NJ 07043, USA

DOI: 10.1002/smll.201200240

NANO MICRO small

biochips containing nanochannels enable the sensitive analysis of DNA molecules. These nanofluidic systems have the capacity to probe the conformational, dynamic, and entropic properties of DNA molecules; they are also able to rapidly sort DNA molecules and determine the spatial location of genetic information along long DNA molecules.[14] The most important contribution of nanochannels is their applications as biosensors for DNA analysis, which further drives more developments in nanochannel fabrication and integration. In practical biosensor devices, the selection of testing model DNA molecules, fluidics and data analysis are also very important for the visualizing genomic information.[15]

Several good reviews have been already dedicated to the fabrication of nanochannels, nanofluidics (transport, separation, etc.), and biochips for DNA analysis.[16–18] Here, our review focuses on both the fabrication of nanochannels and the demonstration of their DNA analysis applications. We discuss the fundamental flow and transport physics in nanochannels, and then focus on several recent common fabrication approaches for nanochannels and the corresponding nanofluidic biochips for DNA analysis. Finally, we summarize and discuss the future challenges and perspectives for nanochannel-based nanofluidic biochips for the analyses of DNA and other biomolecules.

Deying Xia is a research associate fellow in the Department of Materials Science and Engineering at Massachusetts Institute of Technology. He received his BS in Chemistry from Shandong University in China, and his MS in Chemical Engineering and PhD in Electrical Engineering from University of New Mexico. His research interests include applications of nanotechnology to the fabrication of nanostructures, photonic crystals, biosensors, surface wetting, and microfluidics/nanofluidics.

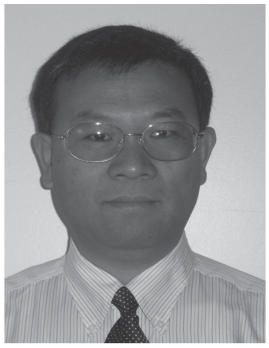

Juchao Yan earned his BS at Jilin University in 1992, and his PhD at Changchun Institute of Applied Chemistry in 1997. From 1998 to 2002, he worked as a postdoctoral fellow and then a research assistant professor at the University of New Mexico. Currently, he is an associate professor of chemistry at Eastern New Mexico University in Portales (New Mexico, USA). His research interests include reagentless electrochemical nanobiosensors, nanochannel-confined lipid bilayers, biofuels, and direct ethanol fuel cells.

Shifeng Hou is currently an Assistant Professor of Chemistry & Biochemistry Department at Montclair State University (New Jersey, USA). He received his BS from Shandong University and his Master's and PhD degrees in electroanalytical chemistry from Nanjing University. He then undertook postdoctoral research for several years and four years industrial development experience as a Senior Research Scientist. His current research area involves electrochemical biosensors, carbon-based nanomaterials, and the application of nanotechnology to environmental protection.

2. Transport in Nanochannels

The evolution from microfluidic to nanofluidic systems has been accompanied by the emergence of new fluid phenomena and the potential for new nanofluidic devices.[10,19] In this section, we briefly review the nanofluidic transport theory by focusing on the various forces that influence the movement of both solvents and solutes through nanochannels.[20] Generally speaking, there are three forces that impact the transport of solutes and solvents through nanochannels: the external driving forces (e.g., an electrical potential gradient or a pressure gradient), the colloidal forces (e.g., electrostatic, van der Waals and hydrophobic interactions), and the friction forces between the wall and the solvent or solute molecules.

We consider an ideally flat wall with no-slip conditions and without surface adsorption. Once such a wall is in contact with an aqueous solution, a surface charge and a local electrostatic potential develop at the interface of the solution and the wall. This potential is screened by a thin layer of adsorbed, immobile counter-ions (i.e., the Stern layer). Because the Stern layer is rarely sufficient to compensate for the initial surface charge, an effective surface charge (σ) is usually considered at the shear plane. This effective surface charge is responsible for a non-zero electrical potential called the zeta potential (ζ), which interacts with ionic species diffusing in the liquid. The mobile diffuse layer, which is outside the shear plane, is where the ions and water molecules can freely diffuse. The Stern layer and the diffuse layer form the electrical double layer (EDL, **Figure 2**). The typical length of an EDL is approximately a few tens of nanometers and is called the Debye length (λ_D). The effective surface charge and the associated EDL have two major consequences in nanochannels: Electro-Osmotic Flow (EOF) and Volumic Surface Charge (C_{VSC}). In nanochannels, axial liquid transport can be induced by applying an axial electric field (E). This field displaces the counter-ions, and drags all of solution inside, resulting in a "plug-like" flow, which is referred to as EOF. The velocity of the EOF (v_{EOF}) is proportional to the zeta potential and, in the Debye-Hückel approximation, to the surface charge:[10]

$$v_{EOF} = -\frac{\varepsilon\zeta}{\eta} E \approx \frac{\sigma\lambda_D}{\eta} E \quad (1)$$

where η is the viscosity and ε is the electrical permittivity of the fluid. C_{VSC} is defined as the ratio of the effective surface charge (σ) to the channel section (S), and can be calculated based on the electro-neutrality of the global system:

$$C_{VSC} = \frac{\sigma}{S} = -\sum_i z_i c_i \quad (2)$$

where c_i is the averaged concentration for the ionic species i of valence z_i. According to Haghiri-Gosnet and co-workers,[19]

DOI: 10.1002/smll.201200240

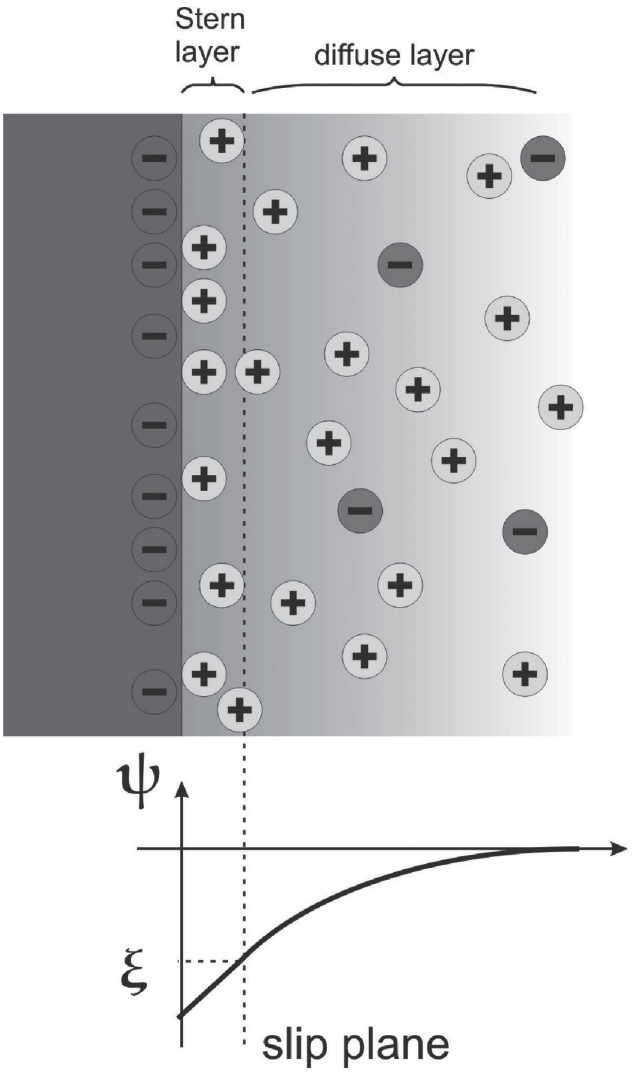

Figure 2. Generally accepted model of the electrical double layer at a solid/liquid interface where cations are specifically adsorbed. Ψ is the electrical potential, and ξ is the zeta potential at the shear plane.[8] Copyright 2008, American Chemical Society.

the modulation of C_{VSC} results in non-linear effects on the ionic transport, which can be used for the simultaneous preconcentration and separation of biomolecules within single, straight channels.

Solvents are transported in nanochannels by an axial pressure gradient (hydrodynamic flow) and/or an axial electrical potential gradient. The average solvent velocity is the sum of the average velocity of the hydrodynamic flow and the average velocity of the electro-osmotic flow.[10] In nanochannels, hydrodynamic pumping is problematic because of the very low average velocity of the hydrodynamic flow. However, electro-osmotic pumping remains viable. Because the electro-osmotic flow velocity only markedly decreases when double layer overlap occurs and when the electrical potential in the double layer approaches the electrical potential in the shear plane. The hydrodynamic flow profile is parabolic, whereas the electro-osmotic flow profile follows the electrical potential profile across the channel.

In nanochannels, the solutes are transported by solvent transport (convection), a solute concentration gradient (diffusion), or an electrical potential gradient (migration) for ions. The solute fluxes that result from these three driving forces are combined in the Nernst-Planck equation

$$J_i = -D_i(\nabla c_i + \frac{z_i q}{kT} c_i \nabla \psi) + c_i u \quad (3)$$

where J_i (mol s^{-1} m^{-2}) and D_i (m^2 s^{-1}) represent the solute flux and the diffusion constant of the ith ionic species, respectively; q (C) is the unit charge; ψ (V m^{-2}) is the electrostatic potential; u (m s^{-1}) is the linear velocity; ∇c_i and $\nabla \psi$ represent the concentration gradient and the electrostatic potential gradient, respectively; and k (J K^{-1}) and T (K) represent Boltzmann's constant and the absolute temperature, respectively.[20] Specific transport phenomena, such as concentration polarization, exist in nanochannels. As a voltage is applied across a nanochannel, ions are rapidly enriched at one end and depleted at the other end of the nanochannel. The degree of enrichment and depletion depends on the extent to which the EDL overlaps. Because of the need to maintain electrical neutrality, the number of cations at both ends is matched by the number of anions, which causes a salt concentration gradient in the diffusion boundary layers on both ends of the nanochannel. Because of this phenomenon known as concentration polarization, the salt concentration increases on the end of the nanochannel and decreases on the other end. Surface conduction is the other transport phenomenon. Because the ionic concentration in the EDL is higher than in the bulk of the liquid, the contribution of the conduction in the double layer, which is known as surface conduction, increases on downscaling.

Wall effects, including slip and specific adsorption, exhibit a pronounced effect on the transport properties.[20] The influence of a non-zero velocity of liquid molecules at the channel wall is known as liquid slip, which is quantified by the slip length. In theory, liquid slip increases the hydrodynamic flow velocity in a nanochannel because it dramatically reduces the required pressure for pressure-driven flows. Once adsorbed on the channel wall, the specifically adsorbed molecules decrease their transport rates. With regard to the diffusion of adsorbing molecules through a nanochannel, the reduced transport rate is accompanied by a sharply defined diffusion front.

In summary, the transport of molecules through nanochannels is affected by the molecular charge, the molecular size with respect to the lateral channel dimensions, and the molecular entropy. Molecules can be excluded from channels by ion exclusion, steric hindrance, and loss of internal entropy. Therefore, nanochannels work as molecular sieves. **Figure 3** shows the three mechanisms of DNA transport in nanochannels.[13] The electrostatic sieving (Figure 3A) is predominant when λ_D is similar to or larger than the typical diameter of the channel. As λ_D becomes negligible, steric and entropic effects become predominant. Ogston sieving (Figure 3B) occurs for DNA molecules that are smaller than the channel. Larger DNA molecules have to unfold to pass through a channel whose diameter is slightly smaller than their diameter of gyration. Thermal agitation allows a loop to escape the entropic trap (Figure 3C).

small 2012,
DOI: 10.1002/smll.201200240

NANO MICRO small

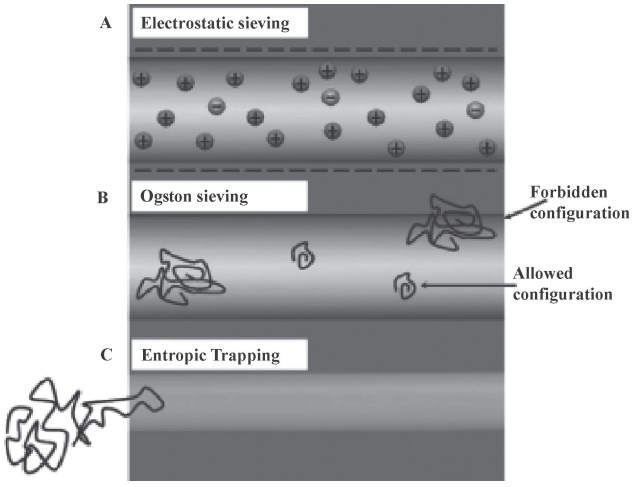

Figure 3. Three different regimes which can be distinguished in nanostructure DNA electrophoresis. The first regime is called electrostatic sieving (A). Here, ions can be selected by using the surface charges and the electrical double layers. In (B), Ogston sieving is presented. Smaller DNA molecules are able to pass through a nanostructure with a higher velocity than larger DNA molecules. In (C), entropic trapping is presented. Entering the confined region requires overcoming an entropic barrier.[13] Copyright 2009, Royal Society of Chemistry.

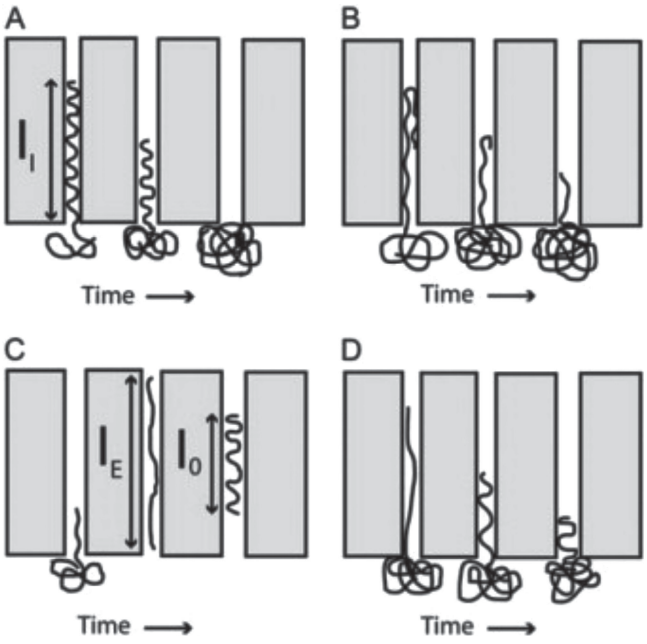

Figure 4. Scehmatic representation of entropic recoiling and relaxation of DNA molecules in nanochannels: (A) self-extraction of a relaxed strand from a nanochannel, driven by the entropic force; (B) unfolding of the looped front end of a molecule during the entropic recoiling process; (C) relaxation of an electrophoretically stretched molecule to its equilibrium extended length (l_0) within a channel; and (D) simultaneous contraction and entropic recoil processes for a molecule which is partially driven into a nanochannel and immediately allowed to recoil.[21] Copyright 2006, Biophysical Society.

Under an applied electric field, a sufficiently long loop can pull the entire molecule inside the channel. As opposed to the sieving mechanisms illustrated in Figure 3, **Figure 4** shows a schematic representation of the entropic recoiling and relaxation of DNA molecules in nanochannels.[21] DNA molecules inserted into a nanochannel array under an applied electric field tend to self-extract themselves from the array when the field is turned off because they experience a confinement-induced entropic force. This effect, termed entropic recoil, was used to sort two different lengths of DNA populations. Craighead and co-workers[21] investigated the motion and conformation of single DNA molecules in 100 nm channels while they were manipulated with both electric fields and confinement-induced entropic forces. By controlling the applied field, they were able to position the molecule as desired, and could observe the conformation of the molecule as it stretched (Figure 4C), relaxed, and recoiled from the nanochannel (Figure 4A). The use of a controlled applied field and the entropic interfacial forces allowed them to unfold molecules (Figure 4B) before they exited the nanochannel. Finally, they also demonstrated that under certain initial conditions it is possible for a molecule to simultaneously undergo both the contraction and entropic recoil processes (Figure 4D).

3. Fabrication of Nanochannels and Their Applications as Biosensors for DNA Analysis

Table 1 summarizes several techniques used to fabricate nanochannels, especially those employed in nanofluidic biochips for DNA analysis. These techniques can be divided into two large categories: top-down and bottom-up methods.[22] Top-down methods are based on lithographically defined patterns that are transferred into underlying layers, whereas bottom-up methods arrange atoms, molecules and particles

Table 1. The summary of typical fabrication methods to form nanochannels.

Fabrication method	Minimum size of channel [nm]	Materials/substrate	Advantage/disadvantage
Conventional photolithography	40–100 in one dimension	Photoresist polymer/silicon(glass)	Easy and accessible, 1D nanoslit, 2D post
Interference lithography	10	Photoresist polymer/silicon(glass)	fast, maskless, arrays of square and deep nanochannels
Electron beam lithography	<5	Photoresist polymer/silicon(glass)	freedom of patterns, small feature size, relatively slow process
Polymer nanochannel	20	Polymer	simple, bottom-up, adjustable, temperature sensitive
Nanoimprint lithography	6–40	Photoresist polymer/silicon(glass)	high throughput, mold/releasing issue, hard to form deep channels

to form nanostructures. Here, we review both the advantages and disadvantages of these methods and provide some future perspectives. It is concluded that the fabrication technology for the region of 1–10 nm is lacking and potentially can be covered using the pulsed-laser deposition way as a controlled way for thin film deposition (thickness of a few nanometers) and further structuring by the top-down method.

With regard to the complexity of fabrication processing, both the self-sealing and sealing methods are used to form the final enclosed nanochannel structures. In the self-sealing method, the sealing is achieved during the processing steps of channel fabrication or during the modification steps. In this method, bottom-up techniques may be used to fabricate the final channels to avoid the sealing step. The sealing materials are the same as those for the channel structures. Self-sealing to create nanochannels is based on polymer channels, nanoparticle deposition and thin film deposition (e.g., sputtering, oxidation, atomic layer deposition and electron-beam evaporation). In thin film deposition, self-sealing results in both the narrowing and sealing of the trenches.

In the sealing method, top-down fabrication techniques may be used to generate open trenches with the combination of nanolithography, etching and polymer removal. In this method, the selected sealing methods depend on the bulk material. The typical sealing methods include anodic, fusion and polymer bonding. Polymer bonding is employed in rapid prototyping and used for plastic substrates. The advantage of this sealing method is that the channels can be easily opened and cleaned. The disadvantage is that the seal can sag into the channels because of the soft material used. In anodic bonding, large electric fields are applied to assist bonding. Anodic binding is usually used for glass and silicon. In fusion bonding, high temperatures are used for glass materials.

3.1. Conventional Photolithography

Conventional photolithography (standard photolithography, optical lithography) is the most widely used method for fabricating nanochannels for DNA analysis. Most of the nanochannels fabricated using conventional photolithography are planar nanochannels (nanoslits). Because planar nanochannels only require nanoscale precision in the single dimension of depth, they may be fabricated using standard photolithographic processes. Photolithography involves the use of light to expose a pattern in a photo-sensitive organic layer spun over a wafer with a mask between the light source and the wafer to define a pattern. The minimum size of feature is limited by the diffraction of light. Conventional photolithography is widely used in the semiconductor industry because it is capable of high high-throughput pattern definition onto wafers. After defining the photoresist patterns, other semiconductor processing steps such as etching are used to transfer the patterns to a desirable layer. The open channel structures will be sealed with some bonding methods, such as anodic bonding or fusion bonding, to form the planar nanochannels for biosensor applications.

The pioneering work for the separation of DNA molecules was performed on planar nanochannel structures with two height structures serving as multiple entropic traps.[23] Hence, the motion and separation of electrophoresed DNA molecules were observed. Inspired by this observation, many similar separation and sensor devices have been developed for DNA separation. One example is the extension of a planar nanochannel structure to a 2D microchannel structure with a micropillar array (post array) for the high speed fractionation of large DNA molecules.[24] In such a bioseparation device, an array of micro-scale posts serve as the sieving matrix, which sorts DNA molecules in different directions according to their molecular masses, much as a prism refracts light of different wavelengths at different angles.

A further experimental study of the DNA sieving process in patterned, periodic nanofluidic filter arrays was also performed.[25] The nanofilter that was used as the model of a pore-constriction system, consisted of an alternating deep region (300 nm) with a confining shallow region (55 nm) (**Figure 5**A). The depth of the shallow region was of the same order of magnitude as the size of the probed DNA molecules. The electrophoretic motion of DNA through this array arose from biased Brownian motion to overcome the periodically modulated free-energy landscape. The field-dependent motion was explained using a kinetic model based on the equilibrium partitioning theory and Kramer's theory. More importantly, their experimental results showed evidence of the crossover from Ogston-like sieving to entropic trapping, which depended on the ratio between the nanofilter constriction size and the size of DNA (Figure 5B). Such dual-height nanochannel structures can also be used to selectively trap and concentrate nanoparticles and viruses.[26]

Afterwards, the experimental setup was improved to further investigate the bioseparation.[27] In this modified nanochannel structure, a micro-fabricated anisotropic sieving structure was produced that consisted of a 2D periodic nanofluidic filter array. The designed structural anisotropy allowed different-sized or -charged biomolecules to follow distinct trajectories, which resulted in more efficient separation. Separation of both DNA and proteins was successfully

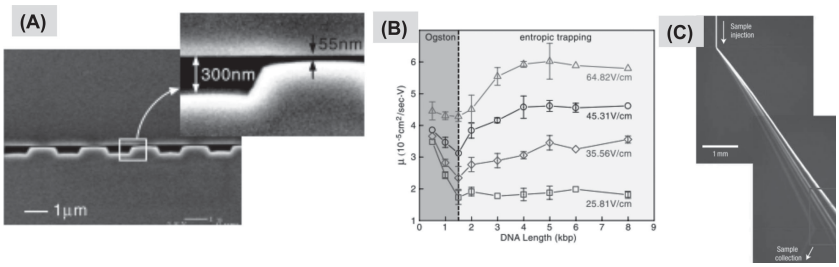

Figure 5. Nanoslits. (A) SEM images of alternating deep (300 nm) and shallow (55 nm) regions with pitch 2 μm; (B) Mobility as a function of DNA length;[25] Copyright 2006, American Physical Society; (C) Fluorescent images show separation of DNA digest at the electric field condition of 185 V/cm^2 for different DNA sizes.[27] Copyright 2007, Nature Publishing Group.

small 2012,
DOI: 10.1002/smll.201200240

NANO MICRO small

achieved using size and electrostatic separation. With the 2D nanofilter system, efficient separation of biologically relevant macromolecules with a broad range of sizes was accomplished in a short period of time. The designed structural anisotropy caused differently sized or charged macromolecules to follow distinct trajectories, which is consistent with either Ogston sieving, entropic trapping or electrostatic sieving (Figure 5C).

Conventional photolithography was combined with etching and bonding to fabricate planar nanochannels (nanoslits) to investigate the electrokinetic concentration of DNA polymers in nanofluidic channels. Both the transport experiments and theoretical modeling revealed the interplay of electrophoresis, electro-osmosis, and the unique statistical properties of confined polymers resulting in the aggregation of DNA. The nanofluidic device with integrated electrodes can preconcentrate DNA at selected locations.

A more complicated nanofluidic device was fabricated using conventional photolithography, etching and anodic bonding to track and manipulate the DNA molecules.[28] The electrodes were implanted inside of the nanochannel. The device structure consisted of two mainstream microchannels interconnected by nanochannels. Once the DNA molecules were trapped within the nanochannel region of the device, it was tracked throughout the length of the channel and the data were recorded and analyzed.

Though conventional photolithography is easily and most often used to produce planar nanochannel structures, it is possible to generate square or nanochannels with an AR of approximately 1 with aid of other processing steps, such as thin film deposition and oxidation. For example, 1D nanochannels were also fabricated using a combination of near-field contact phase-shift lithography and atomic layer deposition.[29] The cross section of 1D nanochannel is triangular with dimensions that are sub-100 nm. The novel combination of these two processes allows for the simple, low-cost, and flexible fabrication of nanochannels comprised of various inorganic materials such as TiO_2. The oxidation of silicon was also used as another facile approach to form nanochannels based on conventional lithography. During oxidation of silicon, the dimension of the microchannels can be reduced to that of nanochannels. Arrays of channels were fabricated using a combination method of photolithography, anisotropic etching, local oxidation of silicon (LOCOS) and sputtering/tilted evaporation.[30] This simple process enables generation of nanochannels for the effective stretching of DNA molecules without the use of nanolithography.

After fabricating planar or square nanochannels using conventional photolithography, the inner wall of the nanochannel can be modified. Layer-by-layer deposition of nanoparticle-containing multilayers offers a simple and powerful pathway to functionalize the nanochannels with nanoporous coatings.[31] Functionalized nanofluidic devices can be used in applications for advanced separations utilizing size, charge, and potentially chemical or biological selectivity. In addition, the nanofluidic systems fabricated using standard photolithography can also be used to detect, separate and pre-concentrate other biomolecules such as proteins.[32]

3.2. Interference Lithography

Standard photolithography techniques can be used to fabricate planar nanochannel structures, but they cannot be used for fabricating square nanochannels and deep nanochannels. In recent years, new nanofabrication approaches have been developed to achieve the goals of further shrinking the dimensions of nanostructures. Interference lithography (IL) is one such nanofabrication method. IL is a powerful nanofabrication method used to generate various periodical nanostructures in large surface areas and flexible patterns with relatively low cost.[33] The IL fabricated nanostructures have demonstrated potential applications in the directed self-assembly of colloidal nanoparticles, nanophotonics, nanoscale epitaxial growth, and nanofluidics. Generally, two or more laser beams interfere to produce periodical patterns on photosensitive layers. Therefore, IL is a maskless technique and can form nanopatterns on different substrates. 1D parallel nanochannel structures and 2D post matrices can be easily fabricated using IL.

The first enclosed nanochannels fabricated using IL were an array of solid parallel channels with anodic bonding to seal the channels.[34] IL and anisotropic dry etching were used to produce large areas of nanoscale parallel grooves. The oxidation of Si was used to further narrow the groove dimensions. Conventional optical lithography was used to create interfacing microchannels. Finally, Pyrex glass was used to seal the grooves to produce nanochannel arrays with anodic bonding. **Figure 6** shows the cross-sectional scanning electron microscope (SEM) images of these structures after plasma etching, oxidation and sealing. After plasma etching, a ~100-nm thick thermal SiO_2 layer was grown to narrow the grooves. A transparent Pyrex cover slip was used to seal the tops of the grooves to form relatively deep nanochannels. The electrokinetic transport in these nanochannels on a series of integrated nano-fluidic chips was studied to control the injection of molecular mixtures into high-density arrays of nanochannels.[35] The electrical field distribution and current leakage in these nanofluidic devices were also investigated in details.[36,37] Furthermore, a fluidic field effect transistor based on these nanochannel structures was fabricated to probe the

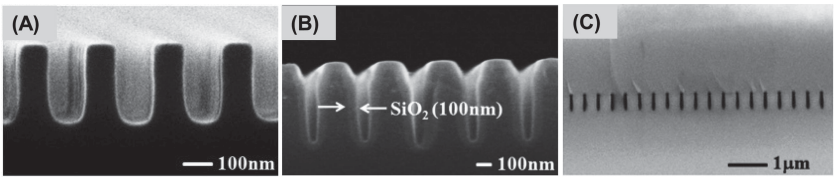

Figure 6. Cross-sectional SEM images of nanochannels: (A) nanochannels after plasma etching; (B) SiO_2-covered nanochannels after thermal oxidation; and (C) nanochannels sealed with a Pyrex cover after anodic bonding.[38] Copyright 2009, Royal Society of Chemistry.

DOI: 10.1002/smll.201200240

transport of charged molecules and to measure the pH shift in nanochannels in response to an electrical potential applied to the gate.[38,39]

An alternative technique of IL to fabricate solid nanochannels with etching and oxidation using IL defined patterns was also developed.[40] Arrays of horizontal nanochannels were produced from the oxidative self-sealing of the grooves after they had been etched in the Si layer. The advantage of this approach is that it can avoid the anodic bonding step and smaller nanochannel arrays can be formed with a relatively long duration of oxidation. The resultant nanochannel exhibited a triangular cross section with an edge length as small as 30 nm. The possible questionable issue arises from the thin sealing layer interfaced with the microchannel section and integration to practical devices.

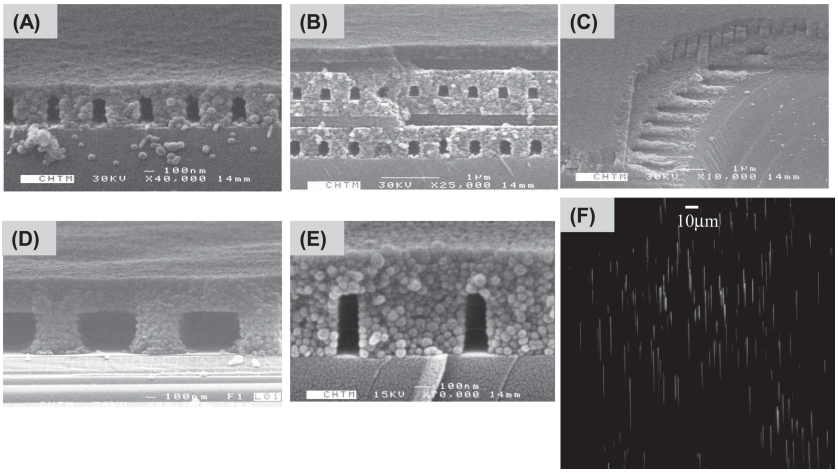

Figure 7. Nanochannels with silica nanoparticles (particle size: 50 nm): (A) one-layer nanochannels; (B) four perpendicular-layered nanochannels; (C) two perpendicular-layered nanochannels; (D) nanoparticle pillar arrays with sealing layer of nanoparticles; (E) narrow nanochannels; and (F) confocal microscope image of DNA in narrow nanochannels as in (E).[41,42] Copyright 2005, American Vacuum Society for (C); Copyright 2008, American Chemical Society for (A,B,D–F).

Another simple approach for fabricating nanochannels using IL was also reported by Xia et al.[41] In this approach, the silica nanoparticle suspension was directly applied on IL-defined photoresist pattern surfaces using spin-coating deposition. Then, high temperature calcination was used to remove the photoresist templates and to enhance the mechanical stability of the nanochannels. The unique characteristic of these as-prepared nanochannels is the porosity in the walls between neighboring channels and the roofs. This novel approach is simple, facile, and fast, and it also avoids the time consuming etching, oxidation and anodic bonding steps that were previously used. Additionally, the porosity of the silica nanoparticles provided separation and transport functionalities. With the use of IL templates, various types of enclosed structures were easily fabricated, including 1D nanochannels, isolated air cavity arrays, post matrices (2D nanochannels) and multilayered nanochannel structures (3D nanochannel structures) with high stability and environmental resistance.[42] Some representative enclosed structures are shown in **Figure 7**. Figure 7A shows the typical porous nanochannels, and Figure 7B-C shows the multilayered nanochannel structures. Figure 7B shows the four-layered perpendicular nanochannels with the same periods in each layer, while Figure 7C shows the two-layered perpendicular nanochannels with different periods in different layers. These 3D nanofluidic systems with multilayer nanochannel structures will be ideal biochip devices that exhibit high efficient separation and multi-component detection. More importantly, as shown in Figure 7D, IL can be used to fabricate post matrices (2D nanochannels). The silica nanoparticle roof is supported by the silica nanoparticle posts, which forms to form 2D nanochannel structures. Figure 7E shows the narrowest nanochannel structures that were obtained using this approach. These nanochannels were continuous along the channel which was verified by fluorescent dye filling and electrokinetic observations. The DNA transport and stretching in the narrow nanochannels are shown in Figure 7F. These porous nanochannels are attractive platforms for studying the fundamental nanofluidic behavior and applications for bioseparation, sensing and detection. Label-free terahertz (THz) transmission measurements were also used in these porous nanochannels to detect RNA molecules.[43] Narrow THz spectral signatures of RNA solution were observed from the nanofluidic channels. This observation was the first demonstration of biosensors with nanofluidic channels for sensing RNA molecules in addition to DNA molecules.

3.3. Electron Beam Lithography

Electron beam lithography (EBL) has been widely used in both the modern semiconductor industries and nanoelectronics. EBL is also an alternative and powerful technique for producing various nanopatterns on surfaces that is often used for fabricating nanochannels and pores; however, it is a time consuming and expensive technique that is not well suited for exposing large areas across an entire wafer due to its serial method. Therefore, EBL is not intensively applied for fabricating nanochannels. However, EBL is a powerful tool for fabricating small or unique nanochannels.

For example, EBL can be used to fabricate a 1D pattern with deep nanochannels on a quartz chip, which can then be used for the separation of DNA.[44] Dry etching was used to transfer EBL defined patterns to the substrates with metal (Ni) mask protection. A thin quartz cover plate was used to seal the open channels, which formed deep nanochannels with bonding. The resulting fabricated nanochannels are 200 nm wide and 5000 nm deep with a 700 nm pitch. This deep nanochannel device was used to separate a mixture of DNA fragments (48.5 kbp and 1 kbp fragments) by applying an electric voltage. It was found that longer DNA

small 2012,
DOI: 10.1002/smll.201200240

NANO MICRO small

fragments migrate faster than shorter ones in this deep nanochannel array chip. The separation behavior is completely different from that with gel electrophoresis or nanopillar chips. Single DNA molecular dynamics from direct observation in the deep nanochannels indicated that both confined elongation and relaxation recoiling of a DNA molecule occur. In addition, an elongated DNA molecule migrates faster than a recoiled DNA molecule. The separation of DNA is governed by the balance between the transverse time and the relaxation-recoiling time.

Additionally, EBL was used to fabricate triangular nanochannels using the collapse of the photoresist layer.[45] Self-sealed nanochannels with triangular cross section shapes are formed from the collapse of hydrogen silsesquioxane (HSQ) resists during the lithography process. Spin coating of extra HSQ layers and thermal curing after initial formation of collapsing triangular structures are used to obtain stable nanochannel arrays for applications in nanofluidic biochips.

In addition, EBL was also employed for the fabrication of sub-10 nm nanochannels.[46] Self-sealing and self-limiting atomic layer deposition (ALD) facilitates the fabrication of lateral type nanochannels that are smaller than the limits of EBL or optical lithography. Highly conformal ALD film structures were used to fabricate lateral sub-10 nm nanochannels with good control over the diameter of the channel. Nanochannel structures that have sub-10 nm dimensions promise to be interesting electrofluidic platforms for studying the motion of single molecules, including DNA.

EBL can also provide excellent control for fabricating complex nanofluidic systems for DNA analysis. For example, EBL was combined with reactive ion etching to produce two orthogonally intersecting arrays of nanochannels with equal pitches and different channel widths in two cross directions on a fused silica wafer that was sealed with a fused silica cover slip.[47] The distinguishing difference between these 2D nanochannel arrays from 2D post matrices is that the distance between nanochannels in 2D nanochannel arrays is much larger than in 2D post matrices. In 2D post matrices (2D nanochannels), the distance between nanochannels is on the same or a smaller order than the channel width, however, in 2D nanochannel arrays, the distance is much larger than the nanochannel width (e.g., a 2 μm pitch with a 100 nm wide nanochannel). A specific DNA orientation and a preferred direction for DNA transport under DC electrophoresis were observed in a square lattice of nanochannels. A change in both the orientation and transport direction was also achieved with application of AC voltage. Complicated, accurate, and controllable DNA analysis becomes feasible with the use of an asymmetric junction of nanochannels.

3.4. Polymer Nanochannels

Glass, fused silica and silicon are the most commonly used substrate materials for the fabrication of nanofluidic devices, due to their established surface chemistry, excellent optical properties, well-developed fabrication technologies and integration in semiconductor processing. However, extensive device processing steps are required in these nanofabrication strategies, and they are therefore limited to the production of low-cost devices. Recently, polymers have provided an alternative to glass-based and silicon-based materials for the fabrication of nanofluidics because of their diverse range of physiochemical properties, low cost, various surface modification possibilities and various available fabrication techniques.[48]

Elastomers are amorphous polymers that have a low to moderate cross-link ratio between polymer chains, whereas thermoplastics are usually linear or branched polymers that have higher molecular weights and Young's moduli. Polydimethylsiloxane (PDMS) is a good example of an elastomeric material, while the typical example of thermoplastics is poly(methyl methacrylate) (PMMA). Both elastomers and thermoplastics are used for the formation of nanochannels and nanoslits, and thus, for the analysis of DNA in these polymer nanochannels.

A direct fabrication method based on tunnel cracking of a readily-prepared brittle layer that is constrained between elastomeric substrates can produce fully-reversible, tunable nanochannel arrays without the use of a molding step.[49] The resulting nanochannels can be adjusted in cross-sections and can be reversibly opened, closed, widened and narrowed by merely applying and removing tensile strains to the substrate. This property permits easy priming or unclogging of the nanochannels for user-friendly and robust operations. The ease of fabrication and operation required to open and close the nanochannels is superior to previous approaches. These arrays of nanochannels are conveniently fabricated using nanoscale fracturing of oxidized PDMS, and can actively manipulate the nanofluidic transport by dynamic modulation of the channel cross-section. The dynamic manipulation of the conformation of single DNA molecules demonstrated the versatility of the elastomeric nanochannels.[50] The ability to modulate entropy dynamically and reversibly opens the doors to investigate and manipulate dynamic behaviors of DNA and other biopolymers at the single-molecule level. Full and partial stretching (13.6 μm) of λ-phage DNA molecules were achieved by applying different pressures. The elastomer nanochannels provide a remarkably versatile example of an actively controlled nanostructure during operation, which can also manipulate various types of nanofluidic transport, bioseparation and biosensing.

Lithography-free fabrication of nanochannel arrays can be fabricated based on cracking process on the surface of polystyrene (PS), which is one type of thermoplastic that is composed of uniaxial macromolecular chains.[51] Under proper conditions, parallel nanochannels (20–200 nm deep, cm long) with equal pitch are obtained. Additionally, PS structures can be successfully copied to PDMS using a plastic mold route, thus making the channel array repeatable and adaptable for further wider applications. These polymer nanochannels are easy to integrate with microchannels for various applications, such as sample pre-concentration or nanofluidic electronics.

The surface wetting properties of polymer nanochannels are extremely important for fluid flow and thus for the analysis of DNA.[52] The surface hydrophilicity of nanochannels can be maintained for at least one month with the use of

DOI: 10.1002/smll.201200240

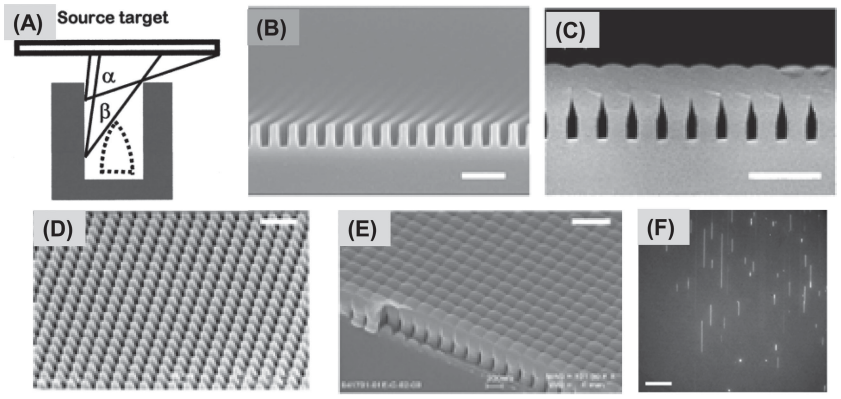

Figure 8. Sputtering sealed nanochannels: (A) a schematic illustration of the sputtering deposition process; (B-C) SEM image of nanochannel structures before and after a single step SiO_2 sputtering (scale bar: 500 nm); (D-E) SEM image of nanopillar array structures before and after sealing by the sputtering process (scale bar: 500 nm); and (F) CCD image of λ-phage DNA concatemers stretched in nanofluidic channels (scale bar: 30 μm).[56] Copyright 2002, American Institute of Physics.

with the use of low-viscosity, thin PDMS layer coatings and oxygen plasma treatment of the cover glass.[53]

Mixed-scale nano- and microfluidic networks were also fabricated in thermoplastics using simple and robust methods, without use of sophisticated equipment to produce the nanostructures.[54] The mixed-scale device could also be used as a master to produce a polymer stamp of PDMS, and used to generate a mixed-scale fluidic network in a single step. Thermal fusion bonding of the cover plate to the substrate at a temperature below their respective glass transition temperatures (T_g) was accomplished using oxygen plasma treatment of both the substrate and cover plate, which significantly reduced thermally induced structural deformation during assembly. The electrokinetic transport properties of double-stranded DNA through the polymeric nanoslits of PMMA were performed. In these polymer devices, the DNA molecules demonstrated field-dependent electrophoretic mobility with intermittent transport dynamics. Different extension factors for DNA molecules were found to have different values for different polymer materials. With further work on this approach, improvements to the degree of extension can be achieved in nanochannels.

3.5. Nanoimprint Lithography

Nanoimprint lithography (NIL) is another good choice for fabricating nanopatterned surfaces as an imprinting and hot embossing technique.[55] With NIL, it is easy to fabricate the nanoscale channels. A 10 nm nanochannel biochip could be easily fabricated using NIL, etching and nonuniform deposition.[56] Similar to most of the nanochannel fabrication methods, parallel nanoscale open channel arrays were formed after etching the NIL defined 1D patterns. Non-uniform deposition was used to seal the open channels and to reduce the dimensions of the enclosed nanochannels. Two approaches were used for the non-uniform deposition: titled electron-beam deposition and sputtering deposition with a large target. **Figure 8** shows several examples of the fabrication of nanochannels and nanopillar arrays (2D nanochannels) using this approach. With regard to the non-uniform deposition, the enclosed nanochannels are well sealed and reach dimensions as small as 10 nm. The initial stretching of DNA was successfully demonstrated in enclosed nanochannels in Figure 8F. Similarly, the thermal oxidation method was used to shrink the nanochannel dimensions.[57] Compared to non-uniform deposition, the oxidation method can produce integrated nanochannel devices that are more robust and reliable. Typically, ultrafast laser melting was first used to seal the etched Si grooves, then the thermal oxidation step was used to further reduce the dimensions of the nanochannels and to modify the inner surface of the nanochannels. Images in **Figure 9** show the 1D and 2D nanochannel structures after etching and laser melting. After laser melting, the formed nanochannels have reduced height compared to before melting. Thermal oxidation can precisely tune the channel size to the sub-10 nm regime. In addition, the oxidation caused the sealing layer to become transparent for DNA fluorescence analysis. **Figure 10** shows the relationship between the of reduced channel size and oxidation time. The

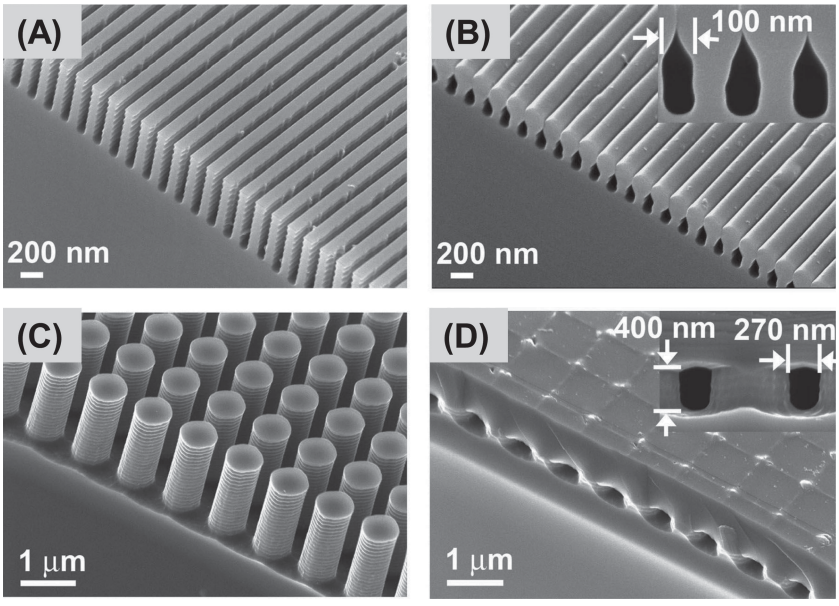

Figure 9. Self-sealing nanochannels: (A) 100 nm wide, 200 nm pitch Si lines (640 nm high); (B) enclosed Si nanochannels after laser pulse; (C) 700 nm diameter Si pillars (970 nm pitch, 2 μm high); and (D) enclosed pillar arrays of channels after laser pulse.[57] Copyright 2008, American Chemical Society.

DOI: 10.1002/smll.201200240

NANO MICRO small

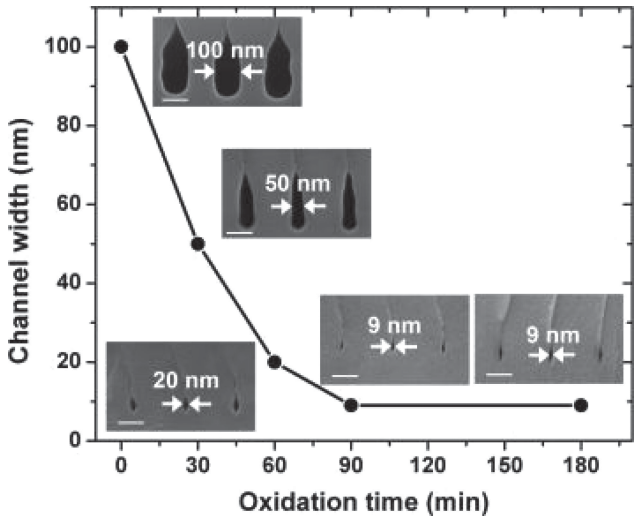

Figure 10. Plot of channel size as a function of wet oxidation time. Insets are the SEM cross sectional images for 100, 50, 20, and 9 nm wide channels, respectively.[57] Copyright 2008, American Chemical Society.

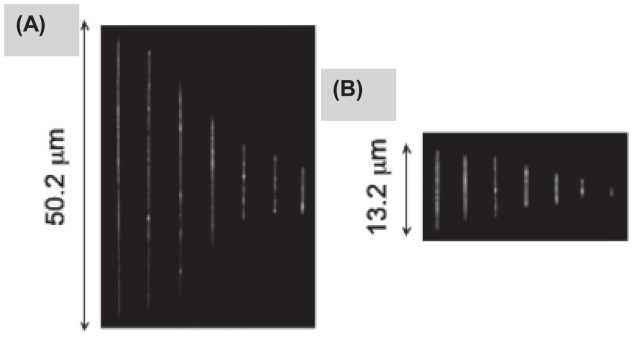

Figure 11. Extended DNA length in different size of nanochannels: (A) averaged intensity of selected T2 DNA molecules in 30 × 40 nm, 60 × 80 nm, 80 × 80 nm, 140 × 130 nm, 230 × 150 nm, 300 × 440 nm, and 440 × 440 nm channels (left to right); and (B) averaged intensity of selected λ-DNA molecules in the same channels.[58] Copyright 2005, American Physical Society.

100 nm wide channels were shrunk to 50, 20, and 9 nm after a 30, 60, and 90 min oxidation, respectively. The cross sectional views of the nanochannels after thermal oxidation appear as droplet shapes. λ-phage DNA molecules were effectively stretched in 20 nm wide nanochannels. As an ultrafast and material selective process, this approach is simple in operation and economical in production.

The structures of NIL-defined nanochannels provide a good platform for studying the statics and dynamics of single DNA molecules that are confined in nanochannels.[58] The nanochannels on fused silica substrate were fabricated with NIL, EBL and quartz bonding to different dimensions.[59] The smart design of nanochannel-based biosensor devices for the manipulation of biopolymers requires an understanding of how the predictions of soft condensed matter physics scale with the dimensions of the nanochannels. DNA stretching was measured at different nanochannel dimensions to show that there is a crossover in the polymer physics below a critical width that is roughly twice the DNA persistence length. **Figure 11** shows images of λ-phage and T2 ds DNA molecules confined in the nanochannels. The stretching of the DNA is clearly a function of the channel width and plateaus as the width drops below the persistence length.

The combination of NIL, etching, thermal oxidation and anodic bonding can be used to fabricate a biosensor device with complex micro- and nano-structures.[60] The nanochannel structure is still the core structure in such a biochip. For example, to develop an innovative single-molecule DNA sequencing device, a two-region device with V-type microchannels before the nanochannel region can provide effective pre-stretching of DNA and control of transport.

NIL was used not only to fabricate the nanochannels in the SiO_2 layer with etching, self-sealing or deposition sealing but also to fabricate the nanochannels in polymer layer.[61,62] The low-cost fabrication of a nanofluidic device with self-enclosed nanochannels that have well-controlled dimensions was achieved in a thin polymer layer in a single step.[61] A high percentage of DNA stretching was observed in the narrow polymer nanochannels. High aspect ratio nanoimprint molds could be fabricated with the combination of anisotropic wet etching and the local oxidation of silicon.[62] NIL was used to create PMMA deep nanotrenches from this unique nanoimprint mold. A novel solvent-assisted sealing technique was developed to seal PMMA nanotrenches. This technique allows the generation of polymer nanochannels with various nanoscale dimensions without the need for complicated and expensive nanolithography tools. **Figure 12** depicts the sparse arrays of deep polymer nanochannels. The initial DNA stretching in these deep polymer nanochannels was observed.

Beyond the arrays of parallel nanochannels, it is a critical challenge to develop nanofluidic biochips with a single, narrow, yet long and continuous fluidic nanochannel at the precisely designated location. Such a single channel can serve as a host for placing electrical or optical sensors inside the nanochannel. Fortunately, novel nanofabrication of imprinted molds for a single channel NIL was creatively developed using a combination of anisotropic etching, conformal coating, and edge patterning.[63] The continuity of the centimeter-long nanochannel was verified by flowing fluorescent dye-stained

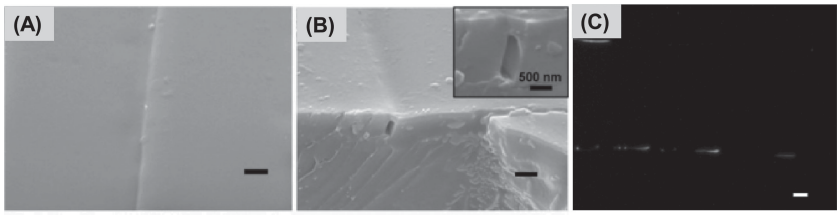

Figure 12. Polymer PMMA nanochannels after solvent-assisted sealing: (A) SEM image of top view (scale bar: 2 μm); (B) SEM images of cross-sectional view (scale bar: 2 μm); and (C) a fluorescent microscopic image of DNA stretched inside two PMMA nanochannels (scale bar: 4 μm).[62] Copyright 2007, Springer.

DOI: 10.1002/smll.201200240

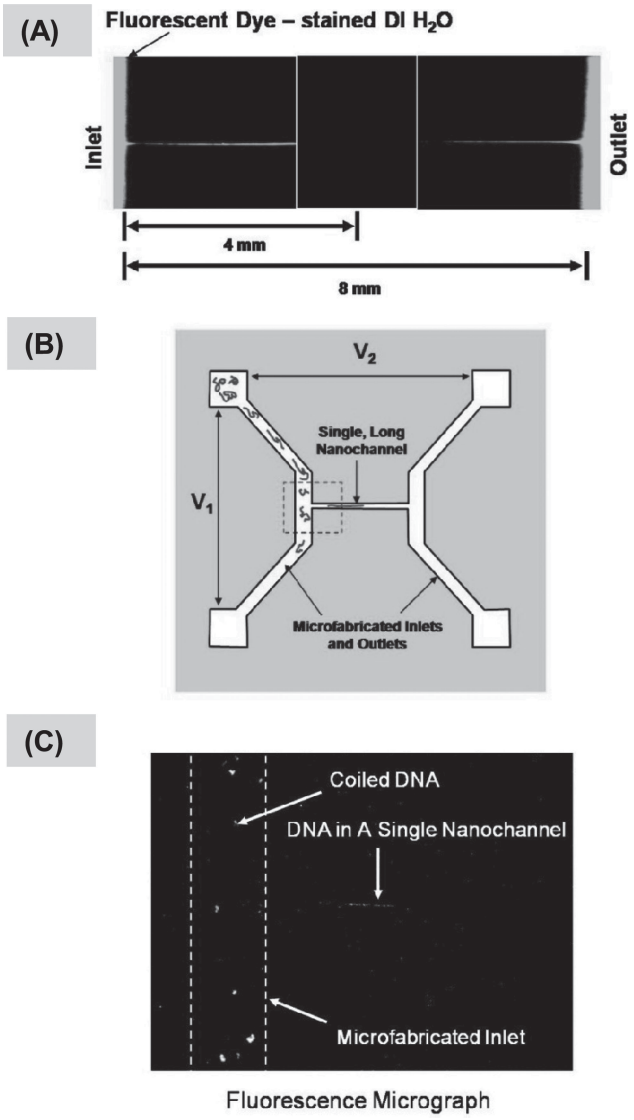

Figure 13. Single nanochannel: (A) continuous water flow with fluorescent dye through a 30 nm wide, 8 mm long single nanochannel; (B) schematic of a single narrow long nanochannel and its inlets and outlets; and (C) a video frame capture of a stretched T2 DNA moving through a 3 mm long, 50 nm square nanochannel driven by electrophoretic force.[63] Copyright 2007, American Chemical Society.

water (**Figure 13**A). The stretching and transporting of DNAs were also demonstrated in such a single nanochannel device, as shown in Figure 13C. Moreover, label-free real-time DNA biosensor was further developed based on a single nanochannel structure.[64] In this biosensor, a long nanochannel was used to stretch a DNA strand, while a nanogap detector inside the channel was used to measure the electrical conduction perpendicular to the DNA backbone as it moves through the gap.

NIL has been shown to be a very useful tool for fabricating the different nanochannel structures. Especially, after the special imprinting mold has been fabricated, the special nanochannel structure will be easily transferred on a Si substrate or polymer layer with NIL. With some treatment methods for formed nanochannels, it is possible to reduce the dimensions of nanochannels into as small as a sub-10 nm feature size.

3.6. Miscellaneous Approaches

Beyond the typical approaches mentioned above, there are other approaches for the formation of special types of nanochannels for some special applications. One example is the use of focused ion beam lithography (FIB) to form a sub-10 nm nanochannel. In FIB lithography, a focused beam of ions (typically Ga) physically sputter neutral and ionized substrate atoms upon impact. 1D nanochannels with critical dimensions extending below 5 nm could be fabricated using FIB milling.[65] Then, the prepared open nanochannels can be sealed with a cover plate; the resulting devices are well-suited for single-molecule DNA transport studies. In addition, this methodology can also be performed using quartz, single-crystal silicon, and PDMS substrates, which demonstrates its general utility. FIB-assisted direct writing and PDMS molds are also used to produce various cross-sectional nanochannel geometries to exploit several DNA manipulation mechanisms such as Ogston sieving, entropic trapping and entropic recoil.[66]

Even though there are many nanolithography techniques available for fabricating the above mentioned nanochannels, the practical biochip devices may be limited by manufacturing cost and yield. Therefore, researchers in this field have focused on and pursued the nanolithography methods with low manufacturing costs. One such nanolithography method is shadow edge lithography (SEL). In SEL, the shadow effect during high vacuum evaporation resulted in the reduction of microstructures to nanostructures. SEL has continuously drawn attention because of its capability for high resolution capability. SEL offers both superior resolution and throughput, which is highly desirable for fabricating nanostructured biosensors. In SEL, the resolution can reach 20 nm for nanochannels across a 100 mm wafer.[67] SEL is superior to other nanolithography methods because it is based on conventional microfabrication techniques.

In addition, block copolymer is also used as a bottom-up, scalable, low-cost, and robust alternative to construct large areas of extremely homogeneous pillared planar nanochannels (2D nanochannels) for nanofluidic applications.[68] This complex hierarchical structure was fabricated using a combination of diverse bottom-up processing strategies (self-assembly of block copolymer, nanostructured sol-gel coatings, highly controlled liquid deposition processing) with powerful top-down techniques (deep X-ray lithography). This unique structure is comprised of mesoporous titanosilicate pillars that are 20 nm in diameter and support a continuous sealing layer of the same material. This structure is a good demonstration of nanopillar matrices with mesoporous materials and shows promising applications for nanofluidics, thus opening the "lab-on-chip" domain to mesofluidics. Other types of materials, such as silica from sol-gel inorganic materials, are also used to form nanofluidic devices for DNA analysis.[69]

The self-assembly of colloidal particles with photonic structures is intensively investigated for many applications,

DOI: 10.1002/smll.201200240

NANO MICRO small

and holds promise for more.[70] The dominant application of photonic crystals is in the optical device. Although DNA-assisted monolayer immobilization of 2D opaline arrays was investigated,[71] there have been few research studies examining DNA separation and sensing using self assembled colloidal photonic structures. Harrison et. al. creatively developed 3D nanofluidic sieves for biomolecule separation.[72] Ordered and robust 3D nanofluidic sieves comprising polystyrene or silica microspheres exhibit fast separation of DNA and proteins. By strict definition, self-assembled 3D photonic structures are easily classified as 1D or 2D nanochannel structures, as they are actually 3D nanofluidic networks. The separation performance of DNA and proteins could be adjusted with precise variation of pore sizes among the photonic structures. This cost effective, bottom-up strategy provides efficient separation of biomolecules.

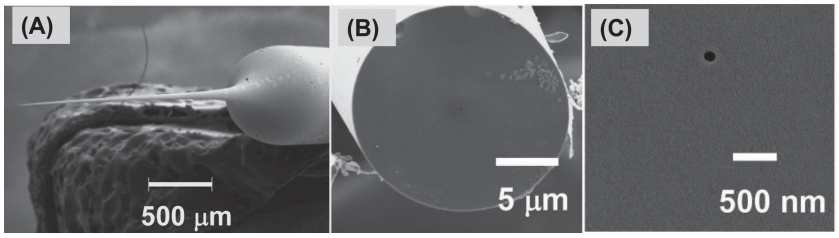

Figure 14. SEM images of silica nanochannel: (A) a silica capillary after being pulled; (B) a 130 nm silica nanochannel: a low-resolution image of the entire tip; and (C) a high-resolution image of the circular opening.[73] Copyright 2009, American Chemical Society.

The NIL is a good top-down approach for the formation of a single nanochannel. Recently, another method for the mechanical preparation of a single channel was developed.[73] The cylindrical-shaped nanochannel was prepared using a simple laser-assisted mechanical pulling process, followed by partial enclosure in a glass micropipette (**Figure 14**). Nanochannels with diameters of 5 to 100 nm can be readily produced from mechanically pulled silica capillary preforms. The advantages of these nanochannels are robust, well-defined geometry, and they are easy to make and to functionalize using silanization process. Molecular transport of DNA molecules through the nanofluidic channels suggests that the transport mechanism of DNA depends on nanochannel sizes (e.g., electroosmotic flow in a 9 nm channel and electrophoretic force in a 75 nm channel).

Sacrificial templates with nanowires to form nanochannels are alternative, simple and low cost methods. In this method, the as-prepared nanowires are first deposited onto a substrate with defined orientations or positions; then some methods are used to apply films to cover and bury the nanowires; finally, the sacrificial templates (nanowires) are selectively removed using suitable methods to form the single nanochannel, arrays of nanochannels or 2D nanochannels. For example, sacrificial electrospun nanofibers can also be used to form nanochannels. After forming electrospun nanofibers on a glass substrate, heat or oxygen plasma are introduced to further reduce the size of the polymer backbone nanofibers.[74] This method uses the scanned electrospinning technique for the generation of oriented sacrificial nanofibers and exposes these nanofibers to harsh, but isotropic etching/heating environments to reduce their cross-sectional dimension to sizes as small as 20 nm. The spin-on-glass (SOG) technique is used to cover and seal the aligned nanofibers. Finally, the sacrificial templates (nanofiber) are removed by calcining at 250 °C. This advancement allows one to fabricate a wider array of more useful nanofluidic devices without complicating the fabrication process. Successful manipulation of single molecules, such as T4 DNA elongation, in the nanochannels was demonstrated. Another example is the formation of polymer nanochannels with silica nanowires as sacrificial templates.[75] Silica nanowire is embedded in the polymer by hot embossing and the silica nanowires are removed using etching with hydrofluoric acid (HF). Various nanostructures, including integrated micro and nanochannels, nanochannel arrays, bent nanochannels and cross-shaped nanochannels were successfully fabricated using this method and were tested with fluorescein sodium solution for applications in nanofluidics. Though the researchers claimed that this technique has the advantages of simplicity and low cost without requiring complicated clean room facilities, we should consider this processing technique to fabricate the nanowires and integrate to nanofluidic system.

Most nanochannels are arranged in horizontal arrays because they are easy to fabricate. However, the layer-by-layer technique can fabricate vertical layered parallel nanochannels. It is challenging to find a facile way to fabricate vertical arrays of nanochannels. Fortunately, vertical arrays of sealed nanofluidic channels with cross-sectional dimensions that are controllable down to 10 nm were fabricated from selective side etching of a SiGe heterostructure comprising layers of alternating Ge fractions, as shown in **Figure 15**.[76] The feasibility of nanochannels for size-based separation of biomolecules was demonstrated by imaging aggregates of tagged peptides. The ability to stack nanochannels one on top of another is highly promising for the subsequent realization of 3D nano-fluidic circuits that are analogous to multi-layer

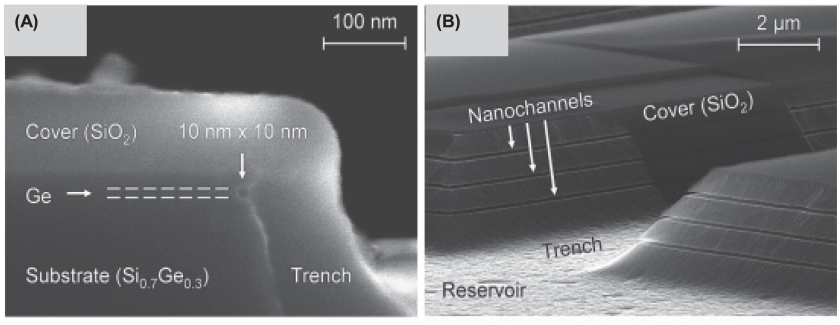

Figure 15. Nanofluidic channels fabricated in two different types of Si-Ge heterostructure: (A) a single nanochannel structure (cross section: 10 nm × 10 nm; and (B) a structure with three nanochannels (cross-section: 130 nm × 100 nm; vertical separation: 500 nm; lateral separation: 480 nm).[76] Copyright 2009, Royal Society of Chemistry.

DOI: 10.1002/smll.201200240

electronic circuits. Biosensors with 3D nanochannel structures are expected to open new vistas for both high throughput biological applications as well as for fundamental studies of complex nanofluidics.

Notably, we have not attempted to cover all methods of forming nanochannels and their applications as nanofluidic biochips for DNA analysis in this review. We expect that more nanochannel fabrication approaches for nanochannels and further advancement in DNA analysis with nanochannels will soon emerge.[77]

4. Conclusion and Perspectives

Compared with other state-of-the-art biosensing platforms, nanofluidic biochips based on nanochannels for DNA analysis are still in their infancy, roughly only one decade old, though they have already shown great promise in the laboratory. Further design and development are expected to lead to a competition with current biosensing methodologies. With rapid advances in nanofabrication in recent years, fabrication methods for nanochannels have already started to deeply impact the improvement and design of highly efficient biochips for DNA analysis. Given the new advances in the fabrication and integration of nanochannels, we believe that the development of low cost, high efficiency, highly sensitive nanochannel-based nanofluidic biochips for DNA analysis is not too distant.

It is expected that understanding the transport of biomolecules, solvents, and ions in nanochannels will be further developed in the near future, as more and more fabrication controls become available for nanofluidic devices. New fluidic physics, including transport and charge mapping, will be proposed to explain the new fluidic phenomena observed in nanofluidic devices. Compared with bulk solutions or microchannels, nanochannels behave differently in terms of liquid slip, chemical equilibrium between solution and wall molecules, adsorption of molecules to the channel walls, and wall surface roughness. The applications of transport in nanochannels range from pumping and transport control to energy conversion and separation. Therefore, a deep understanding of the transport in nanofluidics will be beneficial for designing, controlling and optimizing the nanofluidic biochips with nanochannels, which will improve the sensing capacity and separation efficiency. Based on recent developments, we expect that nanofluidics will play an important role in both fundamental and applied studies of DNA analysis.

This review article has summarized the advancements of nanofluidic biochips based on nanochannels, and has demonstrated the promise of such devices as valuable tools in detecting, sensing and separating DNA molecules. These fabrication methods include, but are not limited to, conventional optical lithography, interference lithography, nanoimprint lithography and polymer instability methods. Each method has its own advantages and limitations. Conventional photolithography is still the most used for nanofluidic studies and planar nanochannel fabrication. In particular, the arbitrary 2D network of planar nanochannels (i.e., having only one dimension in the nanoscale) can be easily attained using photolithography and relatively simple micromachining. NIL and polymer nanochannels are very useful for fabricating square nanochannels, and they are relatively easy to use for producing specific nanochannel profiles. NIL can generate both parallel nanochannels and single nanochannels on different substrates for various biosensing applications. Polymer nanochannels have advantages such as less complicated processing and surface modification to modify the effective sensing. IL is another alternative powerful platform for producing the parallel nanochannels for biosensing devices. In combination with subsequent processing, IL also can push the size of the nanochannels to sub-10 nm. In addition, IL processing easily matchesthe MEMS processing for producing biochips to explore more biosensing applications for a wide range of biomolecules. Slow serial techniques, such as FIB or EBL, have their own advantages towards small nanochannels and are applicable to different substrates. Slow serial techniques can be combined with parallel replication methods (e.g., NIL, IL) to improve their throughput. It has been shown that numerous alternative techniques exist to fabricate 1D nanochannels and 2D networks of straight square nanochannels. A combination of these alternative techniques with the more standard top-down lithography tools may be an elegant solution to pattern arbitrary nanochannels or to prepare nanochannels on other substrates or materials beyond glass, Si and polymer. Finally, the fabrication of deep nanochannels for very dense, high-throughput systems will be further developed in the next couple of years. We also believe more complex nanofluidic systems will also be fabricated to control the fluidic direction, improve the separation efficiency and achieve high throughput sensing.

Despite the progress, several limitations still exist and must be overcome for the integration of nanofluidic biochips based on nanochannels into real applications. These limitations include selectivity, multiplexed detection, and most importantly, the ability to perform field analysis of real-life samples. Once the challenges are overcome, nanofluidic biochips with nanochannels will revolutionize biosensor devices for DNA analysis and for extension to the analysis of other biomolecules such as proteins, viruses and RNA.

Acknowledgements

D. Xia and S. Hou acknowledge the financial support from National Natural Science Foundation of China (21175059). J. Yan acknowledges the financial support from NSF-I/UCRC (0611862), DOE-EPSCoR (DE-FG02-08ER46530) and the Internal Research Grants at Eastern New Mexico University.

[1] B. Gates, Q. Xu, M. Stewart, D. Ryan, C. G. Willson, G. M. Whitesides, *Chem. Rev.* **2005**, *105*, 1171.
[2] H. K. Hunt, A. M. Armani, *Nanoscale* **2010**, *2*, 1544.
[3] Y. Xia, P. Yang, Y. Sun, Y. Wu, B. Mayers, B. Gates, Y. Yin, F. Kim, H. Yan, *Adv. Mater.* **2003**, *15*, 353.

DOI: 10.1002/smll.201200240

[4] I. M. Feigel, H. Vedala, A. Star, *J. Mater. Chem.* **2011**, *21*, 8940.
[5] J. Hahm, C. M. Lieber, *Nano Lett.* **2004**, *4*, 51.
[6] A. Star, J. C. P. Gabriel, K. Bradley, G. Gruner, *Nano Lett.* **2003**, *3*, 459.
[7] K. Balasubramanian, *Biosens. Bioelectron.* **2010**, *26*, 1195.
[8] P. Abgrall, N. T. Nguyen, *Anal. Chem.* **2008**, *80*, 2326.
[9] A. Piruska, M. Gong, J. V. Sweedler, P. W. Bohn, *Chem. Soc. Rev.* **2010**, *39*, 1060.
[10] W. Sparreboom, A. van den Berg, J. C. T. Eijkel, *Nature Nanotechnol.* **2009**, *4*, 713.
[11] H. J. G. E. Gardeniers, *Anal. Bioanal. Chem.* **2009**, *394*, 385.
[12] L. Rassaei, P. S. Singh, S. G. Lemay, *Anal. Chem.* **2011**, *83*, 3974.
[13] G. B. Salieb-Beugelaar, K. D. Dorfman, A. van den Berg, J. C. T. Eijkel, *Lab Chip* **2009**, *9*, 2508.
[14] S. L. Levy, H. G. Craighead, *Chem. Soc. Rev.* **2010**, *39*, 1133.
[15] F. Persson, J. O. Tegenfeldt, *Chem. Soc. Rev.* **2010**, *39*, 985.
[16] J. C. T. Eijkel, A. van den Berg, *Microfluid. Nanofluid.* **2005**, *1*, 249.
[17] Z. Yuan, A. L. Garcia, G. P. Lopez, D. N. Petsev, *Electrophoresis* **2007**, *28*, 595.
[18] J. L. Perry, S. G. Kandkikar, *Microfluid. Nanofluid.* **2006**, *2*, 185.
[19] A. Plecis, A. Pallandre, A.-M. Haghiri-Gosnet, *Lab Chip* **2011**, *11*, 795.
[20] W. Sparreboom, A. van den Berg, J. C. T. Eijkel, *New J. Phys.* **2010**, *12*, 015004.
[21] J. T. Mannion, C. H. Reccius, J. D. Cross, H. G. Craighead, *Biophys. J.* **2006**, *90*, 4538.
[22] D. Mijatovic, J. C. T. Eijkel, A. van den Berg, *Lab Chip* **2005**, *5*, 452.
[23] J. Han, H. G. Craighead, *Science* **2000**, *288*, 1026.
[24] L. R. Huang, J. O. Tegenfeldt, J. J. Kraeft, J. C Sturm, R. H. Austin, E. C. Cox, *Nature Biotechnol.* **2002**, *20*, 1048.
[25] J. Fu, J. Yoo, J. Han, *Phys. Rev. Lett.* **2006**, *97*, 018103.
[26] M. N. Hamblin, J. Xuan, D. Maynes, H. D. Tolley, D. M. Belnap, A. T. Woolley, M. L Lee, A. R. Hawkins, *Lab Chip* **2010**, *10*, 173.
[27] J. Fu, R. B. Schoch, A. L. Stevens, S. R. Tannenbaum, J. Han, *Nat. Nanotechnol.* **2007**, *2*, 121.
[28] V. R. S. S. Mokkapati, V. D. Virgilio, C. Shen, J. Mollinger, J. Bastemeijer, A. Bossche, *Lab Chip* **2011**, *11*, 2711.
[29] F. Guder, Y. Yang, M. Kruger, G. B. Stevens, M. Zacharias, *ACS Appl. Mater. Interfaces* **2010**, *2*, 3473.
[30] Y. H. Cho, S. W. Lee, B. J. Kim, T. Fujii, *Nanotechnology* **2007**, *18*, 465303.
[31] J. Y. Kim, J. P. DeRocher, P. Mao, J. Han, R. E. Cohen, M. F. Rubner, *Chem. Mater.* **2010**, *22*, 6409.
[32] Y.-C. Wang, A. L. Stevens, J. Han, *Anal. Chem.* **2005**, *77*, 4293.
[33] D. Xia, Z. Ku, S. C. Lee, S. R. J. Brueck, *Adv. Mater.* **2011**, *23*, 147.
[34] M. J. O'Brien II, P. Bisong, L. K. Ista, E. M. Rabinovich, A. L. Garcia, S. S. Sibbett, G. P. Lopez, S. R. J. Brueck, *J. Vac. Sci. Technol. B* **2003**, *21*, 2941.
[35] A. L. Garcia, L. K. Ista, D. N. Petsev, M. J. O'Brien II, P. Bisong, A. A. Mammoli, S. R. J. Brueck, G. P. Lopez, *Lab Chip* **2005**, *5*, 1271.
[36] Y. Zhang, T. C. Gamble, A. Neumann, G. P. Lopez, S. R. J. Brueck, D. N. Petsev, *Lab Chip* **2008**, *8*, 1671.
[37] Y.-J. Oh, T. C. Gamble, D. Leonhard, C.-H. Chung, S. R. J. Brueck, C. F. Ivory, G. P. Lopez, D. N. Petsev, S. M. Han, *Lab Chip* **2008**, *8*, 251.
[38] Y.-J. Oh, A. J. Garcia, D. N. Petsev, G. P. Lopez, S. R. J. Brueck, C. F. Ivory, S. M. Han, *Lab Chip* **2009**, *9*, 1601.
[39] Y.-J. Oh, D. Bottenus, C. F. Ivory, S. M. Han, *Lab Chip* **2009**, *9*, 1609.
[40] X. Chen, R. Ji, M. Steinhart, A. Milenin, K. Nielsh, U. Gosele, *Chem. Mater.* **2007**, *19*, 3.
[41] D. Xia, S. R. J. Brueck, *J. Vac. Sci. Technol. B* **2005**, *23*, 2694.
[42] D. Xia, T. C. Gamble, E. A. Mendoza, S. J. Koch, X. He, G. P. Lopez, S. R. J. Brueck, *Nano Lett.* **2008**, *8*, 1610.
[43] E. R. Brown, E. A. Mendoza, D. Xia, S. R. J. Brueck, *IEEE Sens. J.* **2010**, *10*, 755.
[44] T. Yasui, N. Kaji, R. Ogawa, S. Hashioka, M. Tokeshi, Y. Horiike, Y. Baba, *Anal. Chem.* **2011**, *83*, 6635.
[45] S. Choi, M. Yan, I. Adesida, *Appl. Phys. Lett.* **2008**, *93*, 163113.
[46] S.-W Nam, M.-H. Lee, S.-H. Lee, D.-J. Lee, S. M. Rossnagel, K.-B. Kim, *Nano Lett.* **2010**, *10*, 3324.
[47] R. Riehn, R. H. Austin, J. C. Sturm, *Nano Lett.* **2006**, *6*, 1973.
[48] R. Chantiwas, S. Park, S. A. Soper, B. C. Kim, S. Takayama, V. Sunkara, H. Hwang, Y.-K. Cho, *Chem. Soc. Rev.* **2011**, *40*, 3677.
[49] K. L. Mills, D. Huh, S. Takayama, M. D. Thouless, *Lab Chip* **2010**, *10*, 1627.
[50] D. Huh, K. L. Mills, X. Zhu, M. A. Burns, M. D. Thouless, S. Takayama, *Nature Mater.* **2007**, *6*, 424.
[51] B. Xu, J. Xu, X. Xia, H. Chen, *Lab Chip* **2010**, *10*, 2894.
[52] D. Xia, L. M. Johnson, G. P. Lopez, *Adv. Mater.* **2012**, *24*, 1287.
[53] S. H. Kim, Y. Cui, M. J. Lee, S.-W. Nam, D. Oh, S. Kang, Y. S. Kim, S. Park, *Lab Chip* **2011**, *11*, 348.
[54] R. Chantiwas, M. L. Hupert, S. R. Pullagurla, S. Balamurugan, J. Tamarit-Lopez, S. Park, P. Datta, J. Goettert, Y. K. Cho, S. A. Soper, *Lab Chip* **2010**, *10*, 3255.
[55] S. Y. Chou, P. R. Krauss, P. J. Renstrom, *Appl. Phys. Lett.* **1995**, *67*, 3114.
[56] H. Cao, Z. N. Yu, J. Wang, J. O. Tegenfeldt, R. H. Austin, E. Chen, W. Wu, S. Y. Chou, *Appl. Phys. Lett.* **2002**, *81*, 174.
[57] Q. Xia, K. J. Morton, R. H. Austin, S. Y. Chou, *Nano Lett.* **2008**, *8*, 3830.
[58] W. Reisner, K. J. Morton, R. Riehn, Y. M. Wang, Z. Yu, M. Rosen, J. C. Sturm, S. Y. Chou, E. Frey, R. H. Austin, *Phys. Rev. Lett.* **2005**, *94*, 196101.
[59] J. O. Tegenfeldt, C. Prinz, H. Cao, S. Chou, W. W. Reisner, R. Riehn, Y. M. Wang, E. C. Cox, J. C. Sturm, P. Silberzan, R. H. Austin, *Proc. Natl. Acad. Sci. USA* **2004**, *101*, 10979.
[60] E. Abad, A. Juarros, A. Retolaza, S. Merino, R. Marie, A. Kristensen, *Microelectron. Eng.* **2011**, *88*, 300.
[61] L. J. Guo, X. Cheng, C.-F. Chou, *Nano Lett.* **2004**, *4*, 69.
[62] Y. H. Cho, J. Park, H. Park, X. Cheng, B. J. Kim, A. Han, *Microfluid. Nanofluid.* **2010**, *9*, 163.
[63] X. Liang, K. J. Morton, R. H. Austin, S. Y. Chou, *Nano Lett.* **2007**, *7*, 3774.
[64] X. Liang, S. Y. Chou, *Nano Lett.* **2008**, *8*, 1472.
[65] L. D. Menard, J. M. Ramsey, *Nano Lett.* **2011**, *11*, 512.
[66] B. Salieb-Beugelaar, E. Angeli, C. Manneschi, L. Repetto, G. Firpo, U. Valbusa, *Lab Chip* **2011**, *11*, 2605.
[67] J. G. Bai, W.-H. Yeo, J.-H. Chung, *Lab Chip* **2009**, *9*, 449.
[68] M. Faustini, M. Vayer, B. Marmiroli, M. Hillmyer, H. Amenitsch, C. Sinturel, D. Grosso, *Chem. Mater.* **2010**, *22*, 5687.
[69] M. B. Mikkelsen, A. A. Letailleur, E. Sondergard, E. Barthel, J. Teisseire, R. Marie, A. Kristensen, *Lab Chip* **2012**, *12*, 262.
[70] J. F. Galisteo-Lopez, M. Ibisate, R. Sapienza, L. S. Froufe-Perez, A. Blanco, C. Lopez, *Adv. Mater.* **2011**, *23*, 30.
[71] S. Kim, B. Yang, S. Hou, J. Lee, F. Papadimitrakopoulos, *Adv. Funct. Mater.* **2006**, *16*, 1590.
[72] Y. Zeng, D. J. Harrison, *Anal. Chem.* **2007**, *79*, 2289.
[73] B. Zhang, M. Wood, H. Lee, *Anal. Chem.* **2009**, *81*, 5541.
[74] S. Park, Y. S. Huh, K. Szeto, D. J. Joe, Jun Kameoka, G. W. Coates, J. B. Edel, D. Erickson, H. G. Craighead, *Small* **2010**, *6*, 2420.
[75] L. Zhang, F. Gu, L. Tong, X. Yin, *Microfluid. Nanofluid.* **2008**, *5*, 727.
[76] R. Sordan, A. Miranda, F. Traversi, D. Colombo, D. Chrastina, G. Isella, M. Masserini, L. Miglio, K. Kern, K. Balasubramanian, *Lab Chip* **2009**, *9*, 1556.
[77] *Microfluidics and Nanofluidics Handbook: Chemistry, Physics, and Life Science Principles* (Eds: S. K. Mitra, S. Chakraborty), CRC Press, Taylor & Francis Group, Boca Raton, FL, **2011**.

Received: February 1, 2012
Revised: March 19, 2012
Published online: